ELSEVIER

Journal of Biomechanics 37 (2004) 1215–1221

JOURNAL OF BIOMECHANICS

www.elsevier.com/locate/jbiomech
www.JBiomech.com

Estimation of material elastic moduli in elastography: a local method, and an investigation of Poisson's ratio sensitivity

Timothy P. Harrigan[a,*], Elisa E. Konofagou[b]

[a] *Exponent Failure Analysis Associates, 21 Strathmore Road, Natick, MA 10760, USA*
[b] *Focused Ultrasound Laboratory, Department of Radiology-MRI Research, Brigham and Women's Hospital, Harvard Medical School, Boston, MA, USA*

Accepted 3 December 2003

Abstract

The local material stiffness of tissues is a well-known indicator of pathology, with locally stiffer tissue related to the possible presence of an abnormal growth in otherwise compliant tissue. Elastography is a non-invasive technique for measuring displacement distributions in loaded tissues within a medical imaging context. From these measured displacement fields, estimated for local strain have been made using well-studied techniques, but the calculation of elastic modulus has been difficult. In this study we show a method for estimating local tissue elastic modulus that gives numerically stable and robust results in test cases, and that is numerically efficient. The method assumes the tissue is isotropic and it requires an independent estimate of tissue Poisson's ratio, but the method reaches a stable result when the estimated Poisson's ratio is in error, and the resulting estimates are not very sensitive to the assumed value.

Keywords: Elastography; Poisson's ratio; Elastic modulus; Strain energy; Numerical model

1. Introduction

Material property estimation from elastography has been an objective from the initial development of the technique (Ophir et al., 1999). The essentials of the technique are based on an imaging procedure usually ultrasound or MRI in which reflections or tagged volumes of material are tracked within an image during an imposed or naturally occurring deformation. By tracking small inhomogeneities within the tissue (such as speckle in an ultrasound image, or tagged regions in an MRI image) a deformation field within the region being analyzed can be measured (Kallel et al., 1998). This allows an estimate of local strain to be made, based on a numerical derivative of deformation with position, and the interpretation of these strain fields in tissues is usually made to find areas where the local material modulus is high, which often indicates a pathologic state (Plewes et al., 2000). Many procedures currently used for the estimation of material properties involve intermediate calculation of strain data (Skovoroda et al., 1995; Sumi et al., 1995), often using shear-wave propagation to estimate local material properties (Sandrin et al., 2002; Tanter et al., 2002).

Kallel et al. (1996) developed an elastic modulus estimation technique by minimizing the sum of squared errors between a measured set of displacements and a set of displacements that was from a numerical elasticity model. The technique is numerically difficult, involving the inversion of a large matrix which is ill-conditioned numerically. Our technique is based on a similar minimization algorithm, but the resulting numerical algorithm is simpler and seems more robust.

The method used in this study to estimate elastic moduli is based on minimizing a cost or error function. Minimizing an overall cost function produces local equations for equilibrium, much the way that minimizing overall stored elastic energy can be used to develop the local equations of elasticity. In this report we describe the cost function we developed, and some preliminary results.

*Corresponding author. Tel.: +1-508-652-8574; fax: +1-508-647-1899.
E-mail address: tharrigan@exponent.com (T.P. Harrigan).

0021-9290/$ - see front matter © 2004 Published by Elsevier Ltd.
doi:10.1016/j.jbiomech.2003.12.027

2. Methods

Elastography operates using strains of approximately 1 percent (Ophir et al., 1999). This small strain magnitude limits the material characterization to the tangent modulus of the tissue at the measurement configuration. In addition, given the number of displacement measurements available, as compared to the number of elastic moduli to be estimated, we chose to use an isotropic material model, with density taken as constant within an element, and to assume a constant Poisson's ratio. Using two-dimensional displacement data, this ensures that at least two measurements are used for each modulus estimate. Further work on methods to increase the ratio of measurements to estimates for modulus are underway which may allow more detailed material characterization.

The cost function we use is based on comparing the actual displacements to the displacements in a finite element mesh using a provisional elastic modulus distribution. The difference in displacement is used in an energy expression as follows:

$$\Psi = (v_i - u_i)K_{ij}(v_j - u_j) \tag{1}$$

with v_i the displacements of nodes computed using a finite element model, u_i the measured displacements at the positions corresponding to the nodes in the finite element mesh, and K_{ij} the stiffness matrix in from the finite element mesh. The indices i and j indicate the degrees of freedom within the finite element model. Physically, $(v_i - u_i)$ corresponds to the error between the predicted displacements in the finite element model and the measured displacements. Therefore, the cost function corresponds to minimizing the energy stored in the displacement errors. Since, in any finite element model of elastic bodies, the stiffness matrix K_{ij} is positive-definite, the error function will be positive, and will only be zero when the vector $(v_i - u_i)$ is identically zero.

In this study, we used a power-law relationship between the elastic modulus and an indicator variable, ϕ, as

$$E = E_0\phi^n \tag{2}$$

and we assume that the material Poisson's ratio is the same for all values of elastic modulus.

Using this relationship, and keeping Poisson's ratio fixed as elastic modulus is changed, the finite element mesh can be written as a sum of the stiffness matrices for the individual finite elements as

$$K_{ij} = \sum_e \phi_e^n K_{ij}^e + K_{ij}^u, \tag{3}$$

where K_{ij}^e is the normalized element stiffness matrix for element e (with $\phi = 1$), and K_{ij}^u is the part of the overall finite element stiffness matrix that is not being estimated (i.e. it is unchanged in the numerical estimation process). For reference, the finite element displacements are computed from

$$K_{rs}\, v_r = R_s \tag{4}$$

with R_s the nodal load vector for the finite element model.

To minimize the function ψ, we will use a pseudo-time stepping method, similar to the bone remodeling methodology used in previous work (Harrigan et al., 1998). Specifically, we use

$$\frac{\partial \phi_l}{\partial t} = -\frac{\partial \Psi}{\partial \phi_l} \tag{5}$$

with t the pseudo-time, to minimize ψ. In Eqs. (3) and (5) we are using subscripts e and l to indicate a particular element indicator variable. We use e within the summation for the total stiffness matrix, and l to denote the resulting time-evolution equations for a particular element indicator variable.

The right-hand side of Eq. (5) can be written as

$$\frac{\partial \Psi}{\partial \phi_l} = 2\frac{\partial v_i}{\partial \phi_l}K_{ij}(v_j - u_j) + (v_i - u_i)\frac{\partial K_{ij}}{\partial \phi_l}(v_j - u_j) \tag{6}$$

and using the expression for the overall stiffness matrix in terms of the element stiffness matrices (Eq. (4)) the derivative of the stiffness matrix can be written as,

$$\frac{\partial K_{ij}}{\partial \phi_l} = n\phi_l^{n-1}K_{ij}^l. \tag{7}$$

To get an expression for the derivative of displacements due to changes in indicator variable values we start with the finite element equation for displacements due to load (Eq. (3)). Taking derivatives with respect to one value of ϕ, labeled ϕ_l, gives

$$\frac{\partial R_s}{\partial \phi_l} = n\phi_l^{n-1}K_{rs}^l v_r + \sum_e \phi_e^n K_{rs}^e \frac{\partial v_r}{\partial \phi_l} + K_{rs}^u \frac{\partial v_r}{\partial \phi_l} \tag{8}$$

and since R_s (the loading applied to the tissue) is fixed, this expression can be written as

$$\left(\sum_e \phi_e^n K_{rs}^e + K_{rs}^u\right)\frac{\partial v_r}{\partial \phi_l} = -n\phi_l^{n-1}K_{rs}^l v_r \tag{9}$$

and, defining

$$C_{ts} = \left(\sum_e \phi_e^n\, K_{ts}^e + K_{ts}^u\right)^{-1} \tag{10}$$

we can write

$$\frac{\partial v_t}{\partial \phi_l} = -C_{ts}n\phi_l^{n-1}K_{sr}^l v_r. \tag{11}$$

On substituting into the equation for the derivative of the indicator function (Eq. (8)), and simplifying, we arrive at

$$\frac{\partial \Psi}{\partial \phi_e} = \frac{-n}{\phi_e}[v_i(\phi_e^n K_{ij}^e)v_j - u_i(\phi_e^n K_{ij}^e)u_j]. \tag{12}$$

Physically, the two terms in the bracket on the right-hand side are the strain energy in element e due to

computed and measured displacements, respectively. This allows the minimization of ψ using equation

$$\frac{\partial \phi_e}{\partial t} = \frac{n}{\phi_e}[v_i(\phi_e^n K_{ij}^e)v_j - u_i(\phi_e^n K_{ij}^e)u_j]. \quad (13)$$

To test the ability of the finite element formulation shown above to estimate elastic modulus distributions from displacement distributions, we first studied the simplified loading case shown in Fig. 1. In this case an 8 element by 8 element finite element model was used with the four central elements stiffer than the remaining elements by a factor of three. Plane strain was assumed. Four-noded linearly interpolated elements were used, with loads applied to the uppermost nodes to simulate a uniform tensile stress. The sides of the model were unconstrained, and the bottom of the model in Fig. 1 was constrained so that vertical motion was prevented but horizontal motion was allowed except at the middle node. The displacement distribution u_i for the feasibility study was taken from a linear elastic calculation using the target elastic modulus distribution.

Since the finite element formulation is static and linear, the units and lengths used for the physical variables scale according to well-known characteristics. The region considered was 40 mm × 40 mm. The outer part of the finite element model has an elastic modulus of 100 MPa, and the simulated inclusion has an elastic modulus of 300 MPa. Loads of 1 N were applied to the top corner nodes, and 2 N were applied to the top nodes between the corners. With the assumption of plane strain, and a 1 mm thickness for the plane considered, this corresponds to a stress of 0.4 MPa. Using scaling arguments, these displacements also correspond to the case where the outer material has an elastic modulus of 100 kPa, the inclusion has an elastic modulus of 300 kPa, and the applied loading simulates a uniform pressure of 0.4 kPa. Poisson's ratio for both the inclusion and the surrounding material was taken as 0.4 during the calculations of the target displacement field u_i.

2.1. Stability studies

The method shown above is not guaranteed to find indicator variable values for which the error function shown in Eq. (1) is a minimal value. Given that the indicator function depends on the elastic modulus distribution directly, through the finite element stiffness matrix K_{ij}, and indirectly, through the approximated displacements v_i, the method could either fail to find an equilibrium at all, or it could find an equilibrium that is not a minimum (e.g. a saddle point or a maximum). Small-scale stability studies (involving one or two elements) have been carried out, indicating that taking the exponent "n" in Eq. (2) equal to 1 should result in a stable simulation.

Several simulations were run with the initial modulus distribution nearly equal to the one used to calculate the target displacements, but with small perturbations applied away from the known modulus distribution. This was meant to test the response to perturbations away from a known equilibrium.

2.2. Prediction from a uniform initial state and sensitivity to Poisson's ratio

To assess how well this algorithm can fit elastic modulus distributions that are significantly different

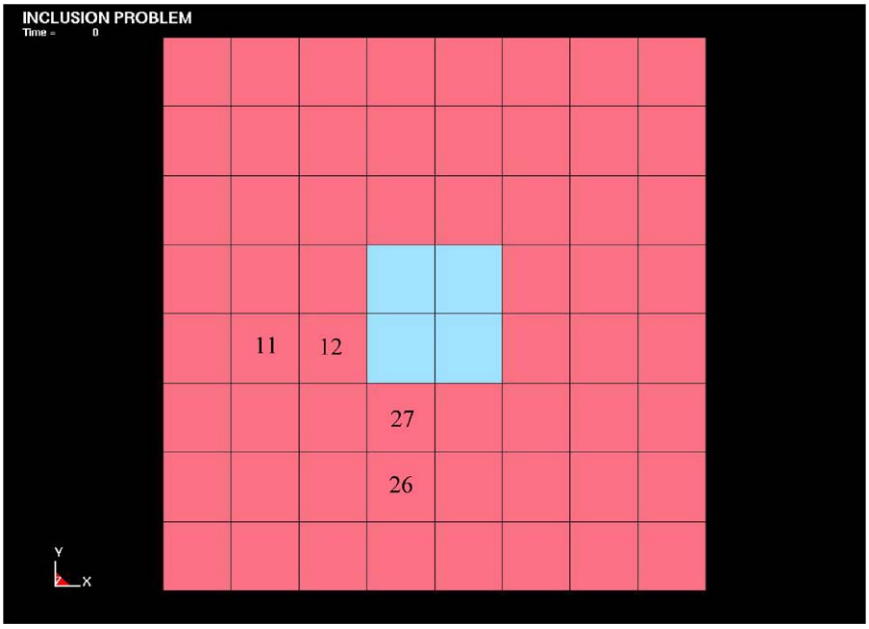

Fig. 1. Finite element mesh used in this study. The indicated element numbers are referred to in Figs. 2 and 7.

from the initial conditions in the calculation, calculations were made using uniform indicator variable distributions as initial conditions. In addition, since the material Poisson's ratios are not part of the fitting process, calculations were carried out to assess whether the results or the stability of the calculations were significantly influenced by the choice of Poisson's ratio in the calculation.

To test how sensitive the results of the elastic modulus estimation are to an assumed value of Poisson's ratio, a series of calculations was carried out using Poisson's ratio values from 0.35 to 0.45 for the calculation of the approximated displacements v_i. Five values of Poisson's were used: 0.35, 0.375, 0.4, 0.425, and 0.45.

Pseudo-time stepping in the calculations was carried out in an Euler forward fashion. That is, the rate of change in each elastic modulus was calculated using Eq. (13) and the elastic modulus at the next time step was calculated by adding the product of the rate of change and the time step size to the elastic modulus at the current time step.

To measure the overall rate of change in elastic modulus, the sum of the square of the rates of change was calculated, and that sum was divided by the number of elements. The square root of that quantity was used to indicate convergence. A convergence tolerance of 10^{-7} was used in each run in this study.

3. Results

In every simulation we ran where the initial elastic moduli were different from the target modulus distribution by small perturbations, the net results were a stable change towards the target distribution. The approach toward the equilibrium slowed (in pseudo-time) as the distribution approached the target. Fig. 2 shows a representative result for ϕ versus time for two elements. The behavior is not monotonic in some regions, but the overall rate indicator decreased monotonically.

The simulations we ran where the initial elastic modulus distribution was uniform were also apparently stable, and the elastic modulus distributions approached the target indicator variable distribution in all regions after initial non-monotonic behavior. That is, transient elastic modulus estimates often increased, then decreased back to a steady state as a function of pseudo-time. Figs. 3–5 show a number of intermediate indicator variable distributions.

The calculations where Poisson's ratio was different from the value used to generate the target displacements showed behavior similar to the calculation where Poisson's ratio matched the value used to generate the target displacements. That is, the pseudo-time stepping was apparently stable, and after an initial transient in some regions, the elastic modulus distribution approximated that used to generate the target displacements. However, the converged elastic modulus distributions depended on the assumed Poisson's ratio in some systematic ways.

Fig. 6 shows the calculated elastic modulus for the inclusion in five cases where Poisson's ratio for the calculation was varied, using the same displacement distribution as a target. Fig. 7 shows similar plots for elements adjacent to the inclusion. As shown in these

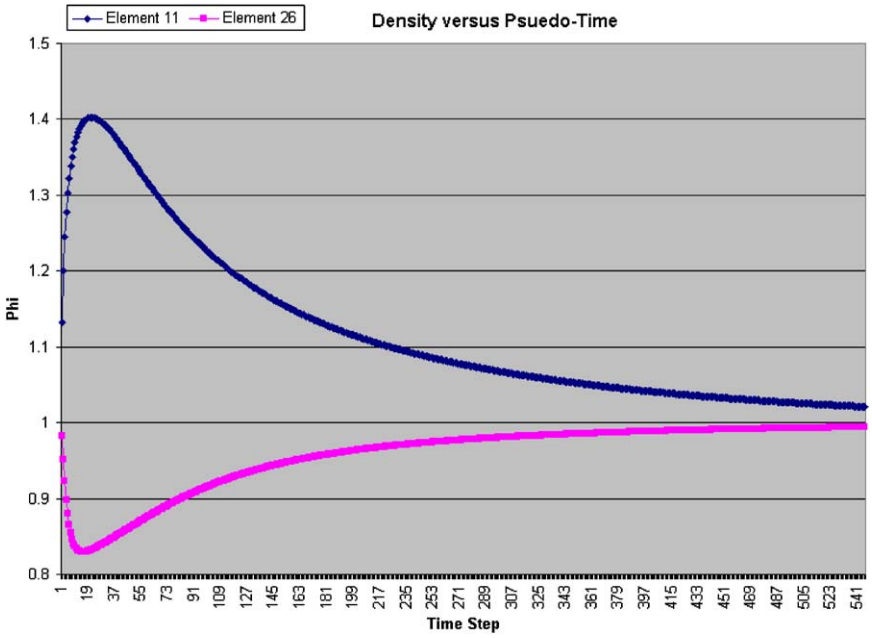

Fig. 2. Representative time histories for element indicator variable calculations in this study. Elements 11 and 26 are shown in Fig. 1.

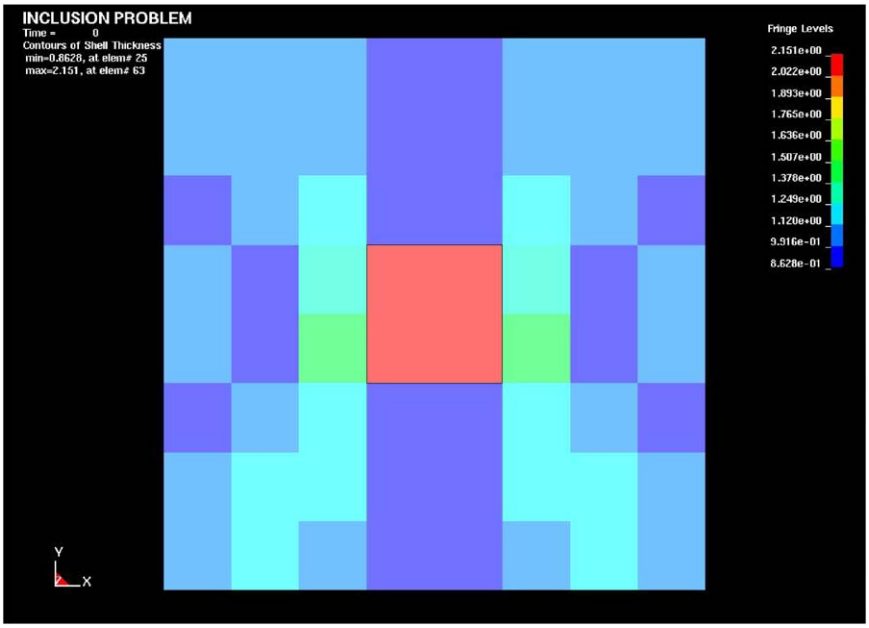

Fig. 3. An indicator variable distribution from relatively early in the iterative calculations. The initial indicator variable distribution in this case was even and taken as 1.0.

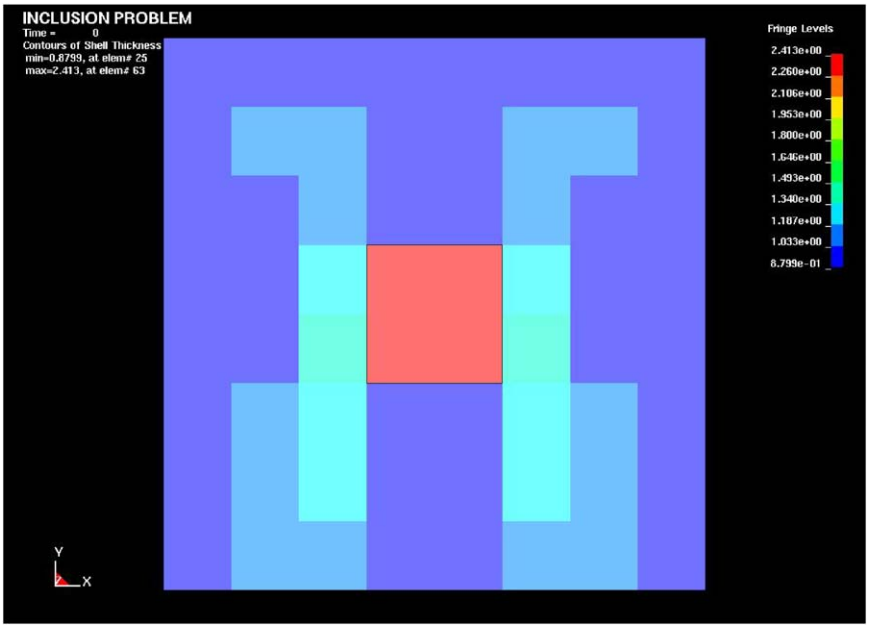

Fig. 4. An indicator variable distribution from later in the iterative calculations. The initial indicator variable distribution in this case was even and taken as 1.0.

plots, the elastic modulus estimates change with the assumed Poisson's ratio, but not in a drastic fashion.

4. Discussion

The method for estimating elastic modulus shown in this study is able to accurately fit a target elastic modulus distribution that mimics an inclusion. The behavior of the fitting algorithm is apparently stable, although a full proof of stability is being investigated.

The method as implemented assumes isotropy and linear elasticity, which is often not present in biological tissues. The assumption of isotropy in this study is motivated by the intent to allow elastic modulus to be estimated for each element. If the elastic modulus of

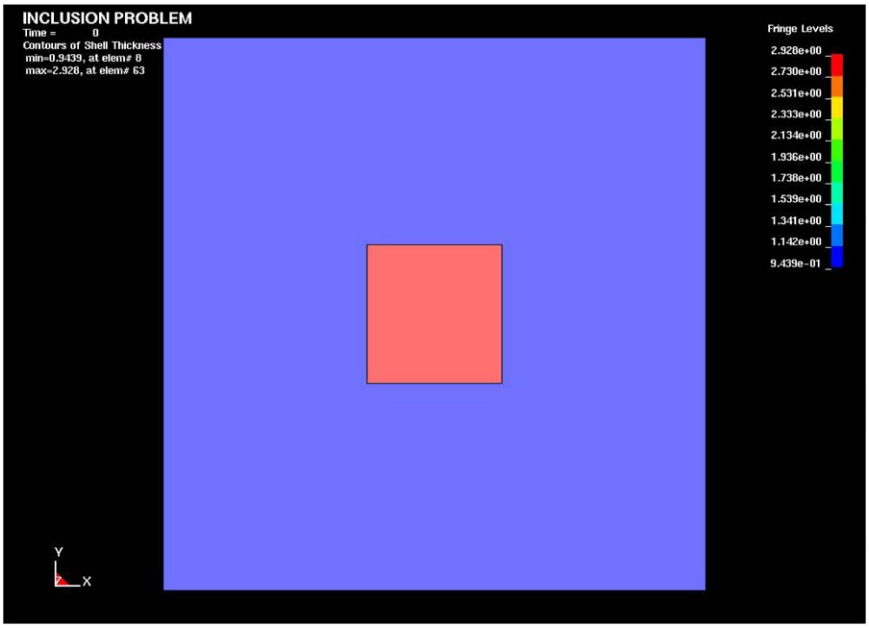

Fig. 5. An indicator variable distribution from late in the iterative calculations. The initial indicator variable distribution in this case was even and taken as 1.0.

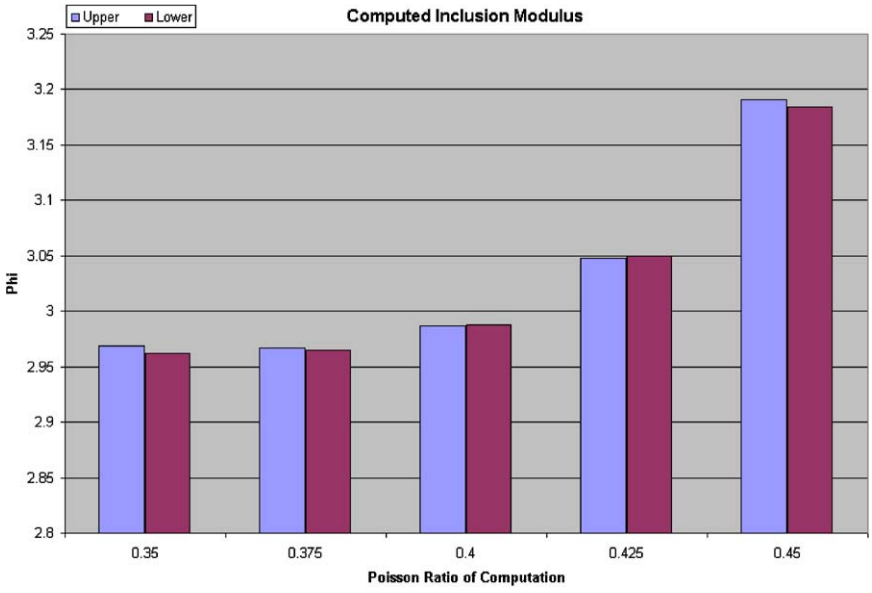

Fig. 6. Long-time estimates of the elastic modulus of the inclusion in this study for a range of assumed Poisson's Ratio. In each case, Poisson's ratio of the entire tissue (inclusion and surrounding material) was assumed to be the value indicated. The bars labeled upper and lower refer to the element position within the inclusion.

each element is estimated, then the number of fitted modulus values is approximately half the number of measured displacements used to estimate these values. An anisotropic material model for each element would require more fitted parameters per element, causing the number of fitted parameters to exceed the number of measurements. The assumption of isotropy could be relaxed if groups of elements were given the same set of modulus values, so that a smaller number of elasticity parameters are estimated from the displacement measurements.

The assumption of linear elasticity limits the method to the estimate of an incremental elastic modulus, since the applied strain in elastography is approximately 1–2 percent, and a linear elastic approach does not allow a measurement of residual stresses or osmotic swelling

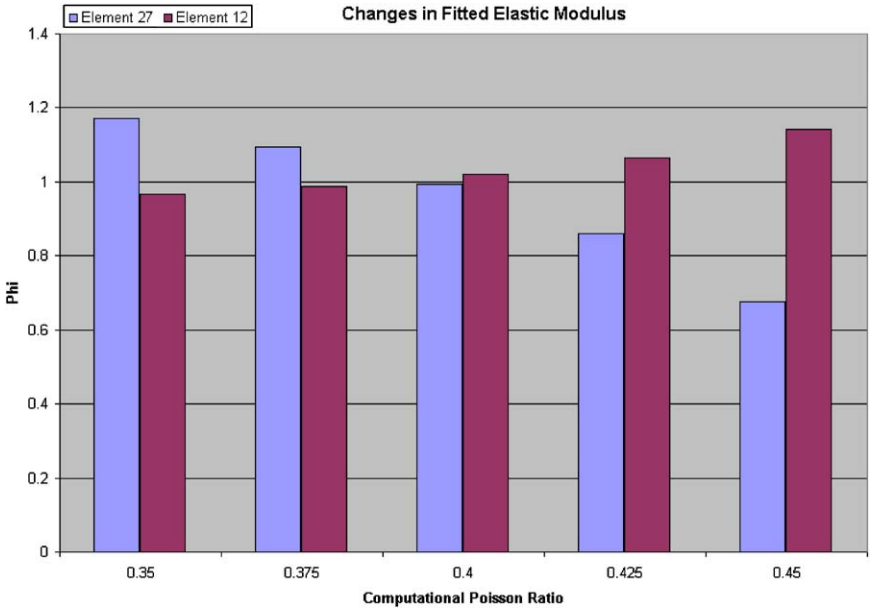

Fig. 7. Long-time elastic modulus estimates of the material surrounding the inclusion in this study for a range of Poisson's ratio. In each case, Poisson's ratio of the entire tissue (inclusion and surrounding material) was assumed to be the value indicated. Elements 12 and 27 are shown in Fig. 1.

effects. However, since changes in incremental modulus with deformation or osmotic swelling are indicative of mechanical or biological events, such as an increasing tension in the connective tissue fibers of the tissue, these incremental elastic properties can be useful for diagnostic purposes.

The elastic modulus fitting algorithm at present employs a value of Poisson's ratio that is set a priori and is not changed during the fitting process. The fitting algorithm arrives at an estimated solution in a manner that is apparently stable even when the computational model uses a Poisson's ratio that is not the same as the one used to compute a target distribution. However, when Poisson's ratio for the computed displacements is significantly different from Poisson's ratio in the material used to generate target displacements, some inaccuracies can result.

Poisson's ratio of most biological tissue is close to 0.5 (nearly incompressible). This may require specialized finite element techniques due to numerical problems, but given the reasonable approximations that can be made with a Poisson's ratio that is different by 0.025 (see Figs. 6 and 7) calculations with Poisson's ratio equal to 0.475 could offer a simple, accurate prediction of elastic modulus as a function of position in elastography. Experiments on measured distributions in phantoms are underway.

References

Harrigan, T.P., Biegler, F.B., Reuben, J.D., 1998. Stability and optimality in bone remodeling simulation. Comments on Theoretical Biology 5 (1), 1–47.

Kallel, F., Bertrand, M., Ophir, J., 1996. Advances in tissue elasticity reconstruction using linear perturbation method. In: Jones, J.P. (Ed.), Acoustical Imaging, Vol. 22. Plenum Press, New York, NY, pp. 267–277.

Kallel, F., Ophir, J., et al., 1998. Elastographic imaging of low-contrast elastic modulus distributions in tissue. Ultrasound in Medicine and Biology 24 (3), 409–425.

Ophir, J., Alam, S.K., et al., 1999. Elastography: ultrasonic estimation and imaging of the elastic properties of tissues. Proceedings of the Institution of Mechanical Engineering [H] 213 (3), 203–233.

Plewes, D.B., Bishop, J., et al., 2000. Visualization and quantification of breast cancer biomechanical properties with magnetic resonance elastography. Physics in Medicine and Biology 45 (6), 1591–1610.

Sandrin, L., Tanter, M., et al., 2002. Shear modulus imaging with 2-D transient elastography. IEEE Transactions on Ultrasonics, Ferroelectrics, and Frequency Control 49 (4), 426–435.

Skovoroda, A.R., Emelianov, S.Y., O'Donnel, M., 1995. Tissue elasticity reconstruction based on ultrasonic displacement and strain images. IEEE Transactions on Ultrasonics, Ferroelectrics, and Frequency Control 42, 747–765.

Sumi, C., Suzuki, A., Nakayama, K., 1995. Estimation of shear modulus distribution in soft tissue from strain distribution. IEEE Transactions on Biomedical Engineering 42 (2), 193–202.

Tanter, M., Bercoff, J., et al., 2002. Ultrafast compound imaging for 2-D motion vector estimation: application to transient elastography. IEEE Transactions on Ultrasonics, Ferroelectrics, and Frequency Control 49 (10), 1363–1374.